



Food availability, but not tidal emersion, influences the combined effects of ocean acidification and warming on oyster physiological performance

Coline Caillon^{a,1}, Elodie Fleury^a, Carole Di Poi^b, Frédéric Gazeau^c, Fabrice Pernet^{a,*}

^a Ifremer, Univ Brest, CNRS, IRD, Laboratoire des Sciences de l'Environnement Marin (LEMAR), 29280 Plouzané, France

^b Ifremer, Univ Brest, CNRS, IRD, Laboratoire des Sciences de l'Environnement Marin (LEMAR), 29840 Argenton-en-Landunvez, France

^c Sorbonne Université, CNRS, Laboratoire d'Océanographie de Villefranche (LOV), 06230 Villefranche-sur-Mer, France

ARTICLE INFO

Keywords:

Air exposure
Food supply
Global change
Multi-stress
Nutrition
Pathogen

ABSTRACT

Many studies on the effects of ocean acidification and warming (OAW) in intertidal mollusks overlook critical factors like tidal emersion and food availability, both of which can shape organisms' responses. Experiments on intertidal bivalves often use constant immersion and abundant food, which likely underestimate global change impacts and underscore the need for more realistic experiments mimicking natural ecosystems. This study investigated the physiological responses of juvenile Pacific oyster *Crassostrea gigas* exposed for 81 days to current and OAW conditions (+3 °C, −0.3 pH units) under two tidal treatments (0 vs. 30 % emersion) and two food levels (ad libitum vs. limited). We measured growth, reproduction, food ingestion, respiration, and biochemical traits like energy reserves and membrane fatty acids. At the experiment's end, oysters were challenged with a viral disease to assess the physiological cost of acclimation and potential trade-offs. Results showed improved oyster physiological performance under OAW with high food level. Nevertheless, food availability emerged as the predominant factor in oyster performance, limiting growth, reproduction, and energy reserves, while increasing oxygen consumption and disease susceptibility. Food deprivation attenuated the beneficial effects of OAW through antagonistic interaction, suggesting physiologically weakened oysters may struggle to adapt to environmental hazards. Finally, tidal treatment had no significant effect, implying that oysters possess physiological compensatory mechanisms, particularly in food acquisition, enabling them to meet nutritional needs during immersion periods. This study provides valuable insights for designing global climate change experiments that align with ecological realism and improves our understanding of the acclimation potential in bivalves facing rapid ocean changes.

1. Introduction

Increasing anthropogenic emissions of carbon dioxide (CO₂) into the atmosphere is resulting in ocean acidification and warming (OAW), thereby endangering marine organisms (Caldeira and Wickett, 2003; IPCC, 2022). Mollusks are particularly susceptible to OAW as several species are sessile for most of their life cycle and therefore cannot escape adverse conditions. As with any ectothermic organism, warming increases the metabolic rates of mollusks until they reach a critical temperature beyond which they can no longer cope (Hochachka and Somero, 2002; Pörtner, 2008). Additionally, ocean acidification (OA) creates corrosive conditions for calcium carbonate (CaCO₃), limiting calcification in mollusks (Gazeau et al., 2013; Orr et al., 2005). The

combined effects of OA and ocean warming (OW) on mollusks can be additive, synergistic, or even antagonistic depending on the species, the life-history stages, and the considered level of change for each driver (Byrne and Przeslawski, 2013; Kroeker et al., 2013; Ross et al., 2024). Simultaneously, marine mollusks continue to face other abiotic and biotic drivers that can interact with OAW, highlighting the need for multiple drivers experiments to better predict the effects of global climate change on marine organisms (Boyd et al., 2018; IPCC, 2022; Riebesell and Gattuso, 2015).

The availability of food, directly influencing the energetic status of organisms, is probably one of the most important drivers in the biological responses of organisms to global climate change (Hettinger et al., 2013; Melzner et al., 2011; Thomsen et al., 2013). For example, mussels

* Corresponding author.

E-mail address: fabrice.pernet@ifremer.fr (F. Pernet).

¹ Present address: Department of Biological Sciences, University of Rhode Island, Kingston, Rhode Island 02881, USA.

reared in low pH and food-limited conditions have reduced growth and more corroded shells than their highly-fed counterparts (Melzner et al., 2011). Very few studies have used half the supply of food to study the responses of oyster larvae under OA and OW conditions (Cole et al., 2016; Parker et al., 2017). The majority of studies investigating the impact of OAW have been conducted under non-limiting food conditions, which may lead to an underestimation of the effects of these processes (Brown et al., 2018; Ramajo et al., 2016). Ad libitum feeding does not accurately reflect natural systems, especially given the potential decline in primary productivity due to global warming, which intensifies ocean stratification and exacerbates drought episodes in coastal areas (Behrenfeld et al., 2006; Fu et al., 2016; Wetz et al., 2011). Both phenomena reduce phytoplankton biomass by limiting nutrient supplies.

Several mollusk species live in the intertidal zone where they are periodically exposed to air during low tide. During these periods, intertidal mollusks stop feeding and their internal pH decreases (Burnett, 1988). The combined pressures of tidal fluctuations and global environmental change may push mollusks beyond their physiological tolerance limits (Helmuth et al., 2006; Scanes et al., 2017). However, most studies investigating the effects of OAW on intertidal species have been conducted under conditions of constant immersion, which may lead to misinterpretation of the experimental outputs. Two studies have explored bivalve responses to OA under varying tidal conditions, and have found that adult intertidal oysters reached their physiological limit (Scanes et al., 2017), while their larvae exhibited greater tolerance to elevated CO₂ (Parker et al., 2021). Failing to consider the native habitats of intertidal organisms represents a critical gap when predicting the impacts of environmental changes on natural coastal ecosystems.

It also appears that in the natural environment, organisms can be exposed to various pathogens, which can become opportunistic when individuals are faced with environmental conditions induced by global change. OA, either alone or in combination with OW, can reduce host immune defenses and increase susceptibility to pathogens (Andreyeva et al., 2024; Bibby et al., 2008; Ellis et al., 2015; Matozzo et al., 2012). These effects may be further exacerbated by additional drivers, such as deoxygenation, changes in food availability and salinity—conditions expected in coastal regions (Rowley et al., 2024). Indeed, increased energy demands to cope with environmental changes can increase susceptibility to infectious disease, as energy is reallocated from immunity to other fitness-related functions (Lochmiller and Deerenberg, 2000; Sokolova, 2013). It is therefore necessary to have the most realistic experimental approach possible when attempting to study the effects of global climate change on marine organisms.

Here, we investigated the combined effects of OA and OW (current vs +3 °C, −0.3 pH units), food availability (high vs low food), and tidal treatment (subtidal vs intertidal) on the physiological performance of the Pacific oyster *Crassostrea gigas*. The Pacific oyster is a globally distributed marine calcifier that preferentially inhabits the upper intertidal zone and is a species of significant economic importance, supporting global fishery and aquaculture industries (Bayne, 2017). After three months of exposure to the different experimental conditions, oysters were challenged with a well-known viral disease that severely hit farmed juveniles every year (Barbosa Solomieu et al., 2015; EFSA, 2015), in order to investigate the physiological cost of acclimation. We hypothesize here that these physiological trade-offs are exacerbated when food availability is limited or when animals are regularly exposed to air.

We examined the biological responses in macro-physiological traits such as growth, reproduction, ingestion, respiration and survival to pathogens. We also measured the energy reserves of oysters which can be involved in energy reallocation due to environmental stress (Sokolova, 2013, 2021). Lastly, we analyzed the composition of membrane fatty acids, a key parameter regulating membrane fluidity, cellular exchange processes, and overall metabolic rates (Hulbert et al., 2007). In summary, our study offers valuable insights for designing

global climate change experiments that align with ecological realism and can be extrapolated to natural systems. Additionally, it enhances our understanding of the acclimation potential in bivalves and the fate of the shellfish industry in a rapidly changing ocean.

2. Materials and methods

2.1. Specimen production and maintenance

Pacific oysters *Crassostrea gigas* were spawned on March 8, 2021 and grown at the Ifremer facilities in Argenton (Finistère, France) and Bouin (Vendée, France) as previously described in Petton et al. (2015). The broodstock consisted of 74 females and 9 males collected in the wild between 2011 and 2018 in Île d'Aix (Charente-Maritime, France; 46°00'40.8"N, 1°09'39.4"W). On May 17, 2021, young oysters were held in a 500-L flow-through tank for four days before the experiment, during which the seawater temperature was gradually increased from 15 to 19 °C. The seawater came from an outdoor pool, which was renewed at each spring tide, filtered through 1 µm and UV-treated. Oysters were fed continuously with the diatom *Skeletonema costatum* (strain CCAP 1077/3), a microalgae widespread in North Atlantic coastal waters and evaluated as a good food source for oysters (Lefebvre et al., 1996; O'Connor et al., 1992). Food concentration was controlled daily using a particle counter (Multisizer 3, Beckman Coulter, Indianapolis, IN, USA; 100 µm aperture tube) and maintained at 1500–2000 µm³ µL⁻¹ at the tank outlet to ensure ad libitum feeding (Petton et al., 2015). On May 21, 2021, at the onset of the experiment, the oysters were 2.5 months old and their mean individual shell length and total mass were 8.4 ± 2.3 mm and 0.11 ± 0.07 g (mean ± s.d., n = 50), respectively. The oysters were screened using a quantitative PCR assay specific to Ostreid Herpesvirus-1 (OsHV-1) at the different stages of production, and no OsHV-1 DNA was detected.

2.2. Experimental design

To investigate the effects of temperature and pH conditions, tidal treatment and food level on the physiological performance of *C. gigas* juveniles, we employed a reduced experimental design (Boyd et al., 2018), which included six conditions: (1) current temperature and pH conditions, subtidal, high food (i.e. reference condition); (2) future OAW conditions, subtidal, high food; (3) current temperature and pH conditions, intertidal, high food; (4) future OAW conditions, intertidal, high food; (5) current temperature and pH conditions, intertidal, low food; (6) future OAW conditions, intertidal, low food. Oysters were exposed to these conditions for 81 days, then sampled for growth, ingestion, oxygen consumption, reproduction, energetics and fatty acid analyses, and further exposed to a pathogenic challenge to assess the physiological cost of acclimation.

2.2.1. Exposure period

The oysters were partitioned into 18 equivalent batches (n = 342 ± 9 individuals; 37.6 ± 0.8 g per batch) and assigned to one of 18 experimental units (see Section 2.3. Experimental setup), which were completely randomized across space. These experimental units corresponded to the six exposure conditions, with each condition having three independent tank replicates.

Current temperature and pH conditions were 20 °C and 7.9 pH units, corresponding to the average sea surface temperature and pH encountered on the French Atlantic coast in summer months (from June to September; Petton et al., 2024). The future OAW conditions represented a scenario of +3 °C and −0.3 pH units projected to occur by the end of the century (SSP3-7.0; IPCC, 2022). The intertidal treatment consisted of 3.5 h emersion twice daily starting at noon and midnight followed by 8.5 h immersion (i.e. ~30 % tidal emersion per day), while the subtidal treatment consisted of constant immersion. This emersion time is relevant to the tidal height at which wild and farmed oysters are found along

the Atlantic coast of France (Pernet et al., 2019a; Walles et al., 2016). During the experiment at low tide, the air temperature surrounding the oysters remained constant over time, thanks to plexiglass lids covering the tanks. Air temperatures were recorded using miniature data loggers placed in the oyster tanks and were 20.0 ± 0.2 and 22.8 ± 0.3 °C (mean \pm s.d., $n = 187$ measurements) in current and future conditions, respectively (C. Caillon, data not shown). The average phytoplankton concentration at the tank outlet was $1451 \pm 538 \mu\text{m}^3 \mu\text{L}^{-1}$ for the high food conditions and $492 \pm 153 \mu\text{m}^3 \mu\text{L}^{-1}$ for the low food conditions. The inlet phytoplankton concentration was progressively increased over time to counterbalance the increasing grazing rate of the growing oysters. The oysters in the high food condition were fed ad libitum, while those in the low food condition were provided just enough to meet their maintenance needs. (Pernet et al., 2019b).

2.2.2. Viral challenge

On August 10, 2021, 1250 oysters (3 kg) from the same initial cohort were myorelaxed in magnesium chloride at 21 °C (Suquet et al., 2009) and injected into the adductor muscle with 100 μL of viral suspension of OsHV-1 μVar (9.3×10^5 copies μL^{-1} diluted by 10 \times). The pathogen donors were then held in a 100-L tank in static oxygenized seawater at 21 °C for 24 h in which they shed viral particles. The seawater surrounding the donors became contaminated with the virus, serving as the source of infection. (Dugeny et al., 2022). The water flow from the infection source constituted approximately 3 % of the total water flow and was delivered directly into the oyster tanks via flexible tubes and a peristaltic pump (Fig. 1). The water supply from the infection source was stopped after 7 days of viral exposure. Survival of oysters was monitored daily for 19 days until mortalities reached a plateau. After 5 days post-infection (5 dpi), when recipient oysters began to die, 10 live oysters were sampled in each tank for OsHV-1 DNA detection and quantification.

2.3. Experimental setup

The experimental flow-through system included 18 independent experimental units consisting of a header tank ($60 \times 40 \times 25$ cm; 45 L), in which 1 μm -filtered and UV-treated seawater was warmed and acidified, connected to a holding tank ($60 \times 40 \times 25$ cm; 45 L) containing the oysters (Fig. 1). The seawater was transferred from the header tank to the holding tank using a water pump (ProFlow t500, JBL, Neuhofen, Germany). Flow rate was adjusted to 500 mL min^{-1} ensuring a complete renewal of the seawater in the holding tank every 90 min. The seawater in oyster tanks was continuously oxygenated and mixed using air bubbling and a circulation pump (ProFlow t300, JBL). The photoperiod was fixed at 14 h light:10 h dark.

The acidified conditions were obtained by pure CO_2 bubbling into the seawater of the header tanks, with the pH level regulated by a pH computer (ProFlora, JBL). Each header tank was also equipped with a thermostat (Biotherm Eco, Hobby, Germany) and heating resistor (Schego Titane 300 W, Europrix, France) to maintain the seawater in the holding tanks at the targeted temperature.

Phytoplankton was delivered directly into the holding tank containing the oysters via flexible tubes and a peristaltic pump (REGLO Analog ISM 827, Ismatec, Glattbrugg, Switzerland). At the inlet, phytoplankton concentration was controlled by adjusting the pump speed. There was one pump per condition combination, for all three replicate tanks. Seawater was sampled daily at the inlet and outlet of each holding tank to measure phytoplankton consumption (in cell volume) using the particle counter.

To simulate tidal emersion, a submersible pump (ProFlow t300, JBL) was connected to an automatic timer (daily programmer TF-6 A, Tibelec, Sainghin-en-Mélantois, France) to drain the water from the oyster tank twice daily. Following the emersion period, the drain pump was automatically turned off and the pump from the header tank slowly refilled the oyster tank.

Seawater effluents from the experimental system were collected in sump tanks and chlorinated for 45 min (12 mg L^{-1} of free chlorine)

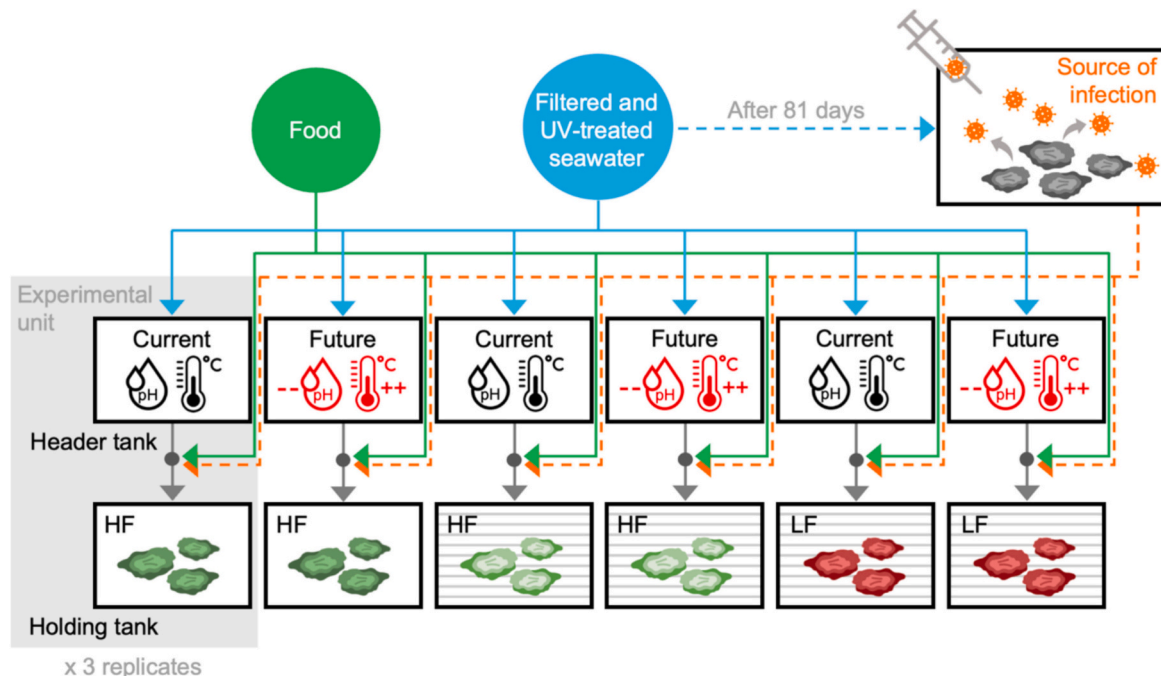


Fig. 1. Experimental design during the 81-day exposure of oysters to six different conditions and the final pathogenic challenge. Arrows indicate the direction of seawater flow. Each experimental unit consists of a header tank, where seawater is heated and acidified, which then flows into a holding tank containing the oysters. Food supply and infection flow are controlled upstream of the holding tank, whereas tidal treatment is controlled within the holding tank. Subtidal treatment (in plain) corresponds to constant immersion (0 % emersion), while intertidal treatment (in striped) corresponds to 8.5 h of immersion followed by 3.5 h of emersion (~30 % emersion). HF, high food; LF, low food.

before neutralization with sodium thiosulfate for 15 min (20 mg L⁻¹).

2.4. Monitoring of seawater physicochemical parameters

Seawater temperature, pH on the total scale (pH_T), dissolved oxygen saturation and salinity were measured daily in holding tanks using a multi-parameter portable meter (MultiLine Multi 3630 IDS – WTW: pH electrode SenTix 940, oxygen sensor FDO 925, conductivity electrode TetraCon 925, Xylem Analytics, Weilheim in Oberbayern, Germany). The pH electrode was verified weekly using Certipur NBS buffers (pH 4.00, 7.00 and 9.00; Merck, Darmstadt, Germany), and then calibrated using a certified Tris/HCl buffer (provided by A. G. Dickson, Scripps Institution of Oceanography, San Diego, CA, USA) to calculate pH values on the total scale (Dickson et al., 2007). Measurements of seawater physicochemical parameters and phytoplankton concentration were taken between 8:00 and 9:00 AM throughout the experiment.

Seawater samples (150 mL) were collected weekly in the holding tanks, filtered through 0.7 µm GF/F glass microfiber filters (Whatman, Florham Park, NJ, USA) and immediately preserved by adding 75 µL of saturated mercuric chloride solution for total alkalinity (A_T) determination. A_T was measured through potentiometric titrations using an automatic titrator (TitroLine 7000, SI Analytics, Mainz, Germany), following the method of Dickson et al. (2007). A_T measurements were performed in triplicate on 25 mL subsamples at 20 °C, with a measurement uncertainty of 0.44 %. Other carbonate system parameters, including partial pressure of CO₂, dissolved inorganic carbon concentration, saturation state with respect to aragonite and calcite, were then calculated from pH_T, A_T, temperature and salinity using the R package *seacarb* (v3.3.1; <https://CRAN.R-project.org/package=seacarb>) (see Table 1).

2.5. Physiological measurements

2.5.1. Growth-related parameters

The total mass of each batch of oysters was measured twice weekly. In addition, the shell length and total body mass (shell + tissue) were measured individually on a subsample of 50 oysters at the start of the experiment (day 0), and on 20 oysters from each tank at the end of the exposure period (81 days). These oysters were dissected and pooled to determine separately the mass of shell and tissue. The tissues were then lyophilized to obtain the dry flesh mass. Growth rate (*G*) was calculated as:

$$G = \frac{\bar{X}_{81} - \bar{X}_0}{81}$$

where *G* is the growth rate expressed as an increase in shell length or total body mass per day (mm d⁻¹ and mg d⁻¹, respectively), and \bar{X}_0 and \bar{X}_{81} are the mean values measured at the onset of the experiment (day 0) and at 81 days. The measurements were done on different individuals between day 0 and day 81.

Table 1

Summary of seawater physicochemical parameters during the 101-day experiment, including the exposure period and viral challenge. Seawater temperature (T), pH on the total scale (pH_T), dissolved oxygen saturation (DO) and salinity (S) were measured daily (*n* = 101), while total alkalinity (A_T) was measured weekly (*n* = 10). Partial pressure of carbon dioxide (pCO₂), dissolved inorganic carbon concentration (DIC), and the saturation state of aragonite (Ω_A) and calcite (Ω_C) were calculated from pH_T, A_T, T and S using the R package *seacarb* (<https://CRAN.R-project.org/package=seacarb>). Parameters were averaged over time within tanks. Values correspond to means ± s.e.m. (*n* = 3 tanks).

Condition	T (°C)	pH _T	A _T (µmol kg ⁻¹)	DO (%)	S (PSU)	pCO ₂ (µatm)	DIC (µmol kg ⁻¹)	Ω _A	Ω _C
Current temperature and pH conditions									
Subtidal, High food	20.0 ± 0.0	7.89 ± 0.01	2198 ± 5	100.4 ± 0.1	35.2 ± 0.0	614 ± 11	2029 ± 2	1.98 ± 0.03	3.04 ± 0.05
Intertidal, High food	20.0 ± 0.0	7.89 ± 0.00	2173 ± 2	100.0 ± 0.1	35.2 ± 0.0	632 ± 11	2011 ± 4	1.89 ± 0.02	2.91 ± 0.03
Intertidal, Low food	20.0 ± 0.0	7.90 ± 0.00	2225 ± 5	100.2 ± 0.1	35.2 ± 0.0	609 ± 10	2052 ± 4	2.02 ± 0.03	3.11 ± 0.04
Future temperature and pH conditions									
Subtidal, High food	23.0 ± 0.0	7.60 ± 0.00	2130 ± 12	99.2 ± 0.1	35.2 ± 0.0	1226 ± 3	2052 ± 11	1.20 ± 0.01	1.84 ± 0.02
Intertidal, High food	22.9 ± 0.0	7.60 ± 0.00	2063 ± 5	99.5 ± 0.1	35.3 ± 0.0	1187 ± 15	1986 ± 6	1.16 ± 0.01	1.77 ± 0.01
Intertidal, Low food	23.0 ± 0.0	7.60 ± 0.00	2190 ± 3	99.6 ± 0.1	35.2 ± 0.0	1265 ± 12	2112 ± 2	1.23 ± 0.01	1.88 ± 0.02

2.5.2. Ingestion

Seawater was sampled daily at the inlet and outlet of each oyster tank to determine phytoplankton concentrations (see the previous section). Ingestion rate (*I*) was determined as:

$$I = \frac{(C_{in} - C_{out}) \times V_{flow}}{M_{batch}}$$

where *I* is the ingestion rate expressed in mm³ g⁻¹ h⁻¹, *C*_{in} and *C*_{out} are the phytoplankton concentrations (in cell volume) measured with the electronic particle counter at the inlet and outlet of the tank (µm³ µL⁻¹), *V*_{flow} is the water flow rate at the inlet of oyster tanks (mL h⁻¹), and *M*_{batch} is the batch total mass (g). The cell volume of phytoplankton ingested per day (expressed in mm³ g⁻¹ d⁻¹) was also reported, accounting for the immersion time, i.e., the time available for feeding throughout the day (24 vs 17 h immersion for subtidal and intertidal treatments, respectively). Ingestion rates were averaged over the exposure period for each tank.

2.5.3. Oxygen consumption

Oxygen consumption rate (*M*_{O₂}) was measured directly in holding tanks on the entire group of oysters after 77 days of exposure. Oysters were not fed for 18 h prior to the start of oxygen measurements to minimize metabolic disturbances. The general procedure was previously described in Lutier et al. (2022). Oxygen concentrations were measured in each tank at the beginning and end of the incubation period which lasted 1.5 h. *M*_{O₂} was reported on an individual and then standardized to the dry flesh mass estimated from a subsample of 20 oysters in each tank. *M*_{O₂} was calculated as follows:

$$M_{O_2} = \frac{\Delta O_2 \times V}{t \times N \times \left(M \times \frac{DM_{20}}{M_{20}} \right)^{0.8}}$$

where *M*_{O₂} is the mass-specific oxygen consumption rate expressed in mg O₂ g⁻¹ h⁻¹, Δ*O*₂ is the difference in oxygen concentration at the start and end of the 1.5-h incubation period (mg O₂ L⁻¹), *V* is the tank volume (L), *t* is the incubation time (h), *N* is the total number of oysters in the batch, *M* is the average individual mass of the oyster batch (g), $\frac{DM_{20}}{M_{20}}$ is the ratio of dry mass to total mass determined after lyophilization a pool of tissue from 20 oysters, and 0.8 is the allometric coefficient for *C. gigas* (Bougrier et al., 1995). Background values obtained from oyster-free tanks were used to correct the respiration rates.

2.6. Reproduction

At the end of the exposure period, 10 oysters per tank (*n* = 30 individuals per condition) were sampled for histological determination of gonadal development. Cross-section of the visceral mass (2–3 mm thickness) was excised and immediately fixed in modified Davidson's solution at 4 °C for 48 h, then kept in alcohol 70 % at 4 °C. Subsequently,

the sections were dehydrated in ascending ethanol solutions, cleared with xylene, embedded in paraffin wax, and stained with Harry's hematoxylin-eosin, as previously described in Fabioux et al. (2005). The gametogenic stage of each oyster was determined under a light microscope according to a modified scale from Steele and Mulcahy (1999). Stage 0 was undifferentiated or resting phase, with no evidence of gonadal development. Stage I corresponded to the early gonadal development, with follicles filled with oogonia in females, or spermatogonia and spermatocytes in males, but the connective tissue was still very abundant. Stage II defined the advanced gonadal development, with vitellogenic oocytes still attached to the follicle walls in females, or spermatids and spermatozoa with tails oriented toward follicle lumen in males. Finally, stage III characterized oysters that had reached maturity, with ripe gonad ready for spawning (unattached mature oocytes in females, or follicles filled with mature spermatozoa with flagella in males) or post-spawning gonad (follicles partially empty and/or presence of phagocytes).

2.7. Biochemical analyses

Soft tissues of 10 oysters from each tank were collected at 81 days, pooled, flash-frozen in liquid nitrogen, and stored at -80°C . Oysters were then ground to a powder with a ball mill under liquid nitrogen and subsampled for lipid, carbohydrate and protein analyses.

2.7.1. Neutral lipids, carbohydrates and proteins

For lipids, the resulting powder (300 mg) was diluted in 6 mL chloroform-methanol solution (2:1, v/v). Neutral lipids (i.e. reserve lipids) were fractionated into lipid classes and quantified using a high-performance thin-layer chromatography coupled with a scanning densitometer (Automatic TLC Sampler 4 and TLC Scanner 3, respectively, CAMAG, Muttens, Switzerland) as previously described in Pernet et al. (2019b). This method allowed the separation of sterols (ST), alcohols, free fatty acids, triacylglycerols (TAG) and monodacylglycerols. Since TAG are reserve lipids and ST are structural lipids of cell membranes which remain largely unchanged, the TAG:ST ratio was used as an index of the contribution of reserve to structure.

Carbohydrate content was determined according to the colorimetric method described in Dubois et al. (1956). Oyster powder (ca. 50 mg) was homogenized in 2 mL of Milli-Q water using a Polytron PT 2500 E (Kinematica, Malters, Switzerland). Samples (250 μL) were mixed with phenol (500 μL , 5 % m/v) and sulfuric acid (2.5 mL, 98 % v/v), and then incubated for 40 min. Absorbance was recorded at 490 nm using a Cary 60 UV-Vis spectrophotometer (Agilent Technologies, Santa Clara, CA, USA). The total carbohydrate content was determined from a standard calibration curve using pure glucose and expressed in mg g^{-1} fresh tissue.

Proteins were extracted from 450 mg of oyster powder using 3 mL of a lysis buffer [150 mM NaCl (Merck), 10 mM Tris/HCl (Sigma-Aldrich), 1 mM EDTA (Quantum), 1 mM EGTA (Sigma-Aldrich), 1 % Triton X-100 (Bio-Rad), and 0.5 % Igepal (Sigma-Aldrich); pH 7.4 at 4°C] with phosphatase and protease inhibitors [1 % of phosphatase inhibitor cocktail II (Sigma-Aldrich), 2 % NaPPI 250 mM (Sigma-Aldrich), and a tablet of complete EDTA free protease inhibitor cocktail (Roche) in 25 mL of lysis buffer]. The resulting lysates were used to quantify the total protein content using the DC protein assay (Bio-Rad, Hercules, CA, USA), following the method of Lowry et al. (1951). Absorbance was read at 750 nm. Protein concentration was determined by comparison with a standard calibration curve supplied with the kit and expressed in mg g^{-1} fresh tissue.

2.7.2. Membrane fatty acids

A 1-mL aliquot of the sample stored in the chloroform-methanol solution was dried, recovered in chloroform/methanol (98:2, v/v) and placed at the top of a silica gel microcolumn. Neutral lipids were eluted with 10 mL of chloroform/methanol (98:2, v/v), and then polar lipids

were eluted with 15 mL of methanol. Tricosanoic acid (2.3 μg) was added as internal standard. Polar lipids were transesterified with a 3.4 % sulfuric acid in methanol solution at 100°C (Couturier et al., 2020), producing fatty acid methyl esters (FAME) from the fatty acids, and dimethyl acetals (DMA) from the alkenyl chains at the sn-1 position of plasmalogens. The FAME and DMA products were analyzed using a gas chromatograph system with a flame ionization detector (HP - Agilent 6890, Agilent Technologies), equipped with a DB-Wax capillary column (30 m length \times 0.25 mm inner d. \times 0.25 μm film thickness). Fatty acids (FA) were then identified by comparison of retention times with standard mixtures. Each FA was expressed as the relative percentage of its peak area by the total area of all polar FA peaks. The unsaturation index was calculated as the sum of the percentage of each unsaturated FA multiplied by the number of double bonds within that FA.

2.8. Detection and quantification of OsHV-1

Total DNA was extracted from 30 mg of dissected mantle and gills of the live oysters collected at 5 dpi using a Macherey-Nagel's tissue kit (NucleoSpin, ref. 740,952.250). DNA concentration and purity were checked with a Nanodrop spectrophotometer (ND-1000, Thermo Fisher Scientific, Waltham, MA, USA).

The detection and quantification of OsHV-1 DNA within each oyster were performed by droplet digital PCR (ddPCR) method using automated droplet generator and reader (QX200 Droplet Digital PCR System, Bio-Rad). Each ddPCR reaction mixture included 11 μL Bio-Rad ddPCR Supermix for Probes (No dUTP), 2.97 μL sterile Millipore water, 0.99 μL of each 20 μM OsHV1BF and B4 primers, 0.55 μL of 10 μM B probe (Martenot et al., 2010), and then 5.5 μL of DNA sample, for a total reaction volume of 22 μL (assuming a 10 % loss). The QX200 Droplet Generator partitioned each reaction mixture into thousands of nanodroplets by combining 20 μL of the reaction mixture with 70 μL of Bio-Rad oil for probes. The resulting droplet volumes of 40 μL were totally transferred into a ddPCR plate for PCR amplification (C1000 Touch Thermal Cycler, Bio-Rad), using the following cycling protocol: hold at 95°C for 10 min, 40 cycles of 94°C for 30 s, 59°C for 1 min, and a final enzyme deactivation step at 98°C for 10 min, then the plate was kept at 12°C . After processing, droplets from each sample were analyzed individually on the QX200 Droplet Reader. Samples were analyzed without replication, and for each ddPCR plate run, a negative control (nuclease-free water, Millipore) and a positive control containing OsHV-1 DNA (from a dead oyster during viral challenge, diluted 1/1000) were included. The reading of droplets was performed with a threshold fixed at 4000 on the software amplitude scale. Results were expressed in OsHV-1 DNA copy number per mg of fresh tissue.

2.9. Statistical analyses

All statistical analyses were performed using RStudio software (v4.3.2) with alpha set at 0.05 for statistical significance. Generalized linear models (GLM) with Gaussian distribution were used to assess the effect of 'Condition' (fixed factor, 6 levels) on growth-related parameters, ingestion and oxygen consumption rates, energy reserves, membrane fatty acids and viral load (*stats* package, v4.3.2). For viral prevalence, we used a generalized linear mixed-effects model (GLMM) with a binomial distribution with 'Condition' as a fixed factor and 'Tank' as a random factor (*lme4* package, v1.1–35.2). Normality of residuals and homoscedasticity were graphically and statistically checked (Shapiro-Wilk and Levene tests, respectively), and the data were log-transformed when necessary. Subsequent Tukey post-hoc test was used to investigate the pairwise differences between conditions (*multcomp* package, v1.4–25). Where necessary, planned contrasts between group means were used to investigate the main effect of temperature/pH conditions (i.e. scenario) and tidal treatment. To determine differences in stages of gonadal development, we performed multinomial logistic regression with the factor 'Condition' (*rnet* package, v7.3–19) followed

by likelihood ratio test (*car* package, v3.1–2).

In addition, principal component analysis (PCA) was performed on the composition of membrane fatty acids to visualize the effect of condition (*FactoMineR* package, v2.10). One-way permutational multivariate analysis of variance (PERMANOVA) with Euclidian distance was used for statistical analysis of fatty acid profile (*vegan* package, v2.6–4).

Kaplan-Meier survival curves of oysters following virus exposure were plotted for each condition and compared using the Log-Rank test (*survminer* package, v0.4.9). The odds of mortality were analyzed using a mixed-effects Cox model with ‘Condition’ as a fixed factor and ‘Tank’ as a random factor (*coxme* package, v2.2–20). The proportionality of hazards was checked and validated by Schoenfeld residuals.

3. Results

3.1. Future ocean acidification and warming (OAW) accelerate growth and reproduction regardless of emersion

The oysters suffered no mortality under the different experimental conditions during the exposure period. At the end of the exposure period, oysters reared under future OAW were larger, heavier and more sexually mature than their counterparts reared under current conditions and no food limitation, regardless of tidal treatment (Fig. 2A-F and 3; Table S1). However, we found a significant effect of emersion on shell mass, total body mass, growth rate in terms of body mass and dry flesh mass which were reduced under future conditions (Fig. 2C-F). Ingestion

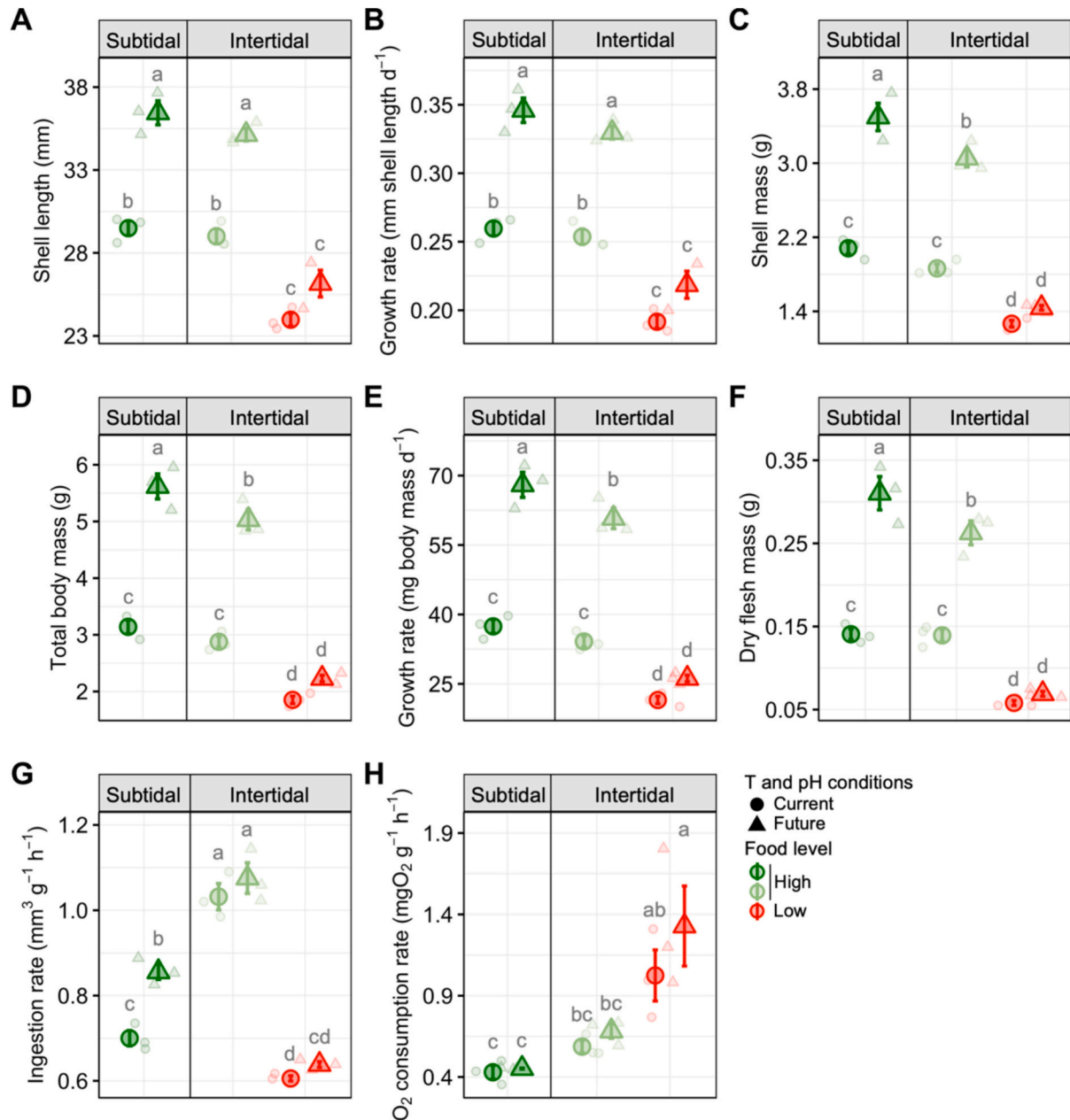


Fig. 2. Physiological parameters of *Crassostrea gigas* oysters under different temperature and pH conditions, tidal treatment and food level during the 81-day exposure period, prior to viral challenge. Specifically, shell length (A), growth rate in terms of shell length (B), shell mass (C), total body mass (D), growth rate in terms of total body mass (E) and dry flesh mass (F) were measured after 81 days of exposure, while ingestion rate (G) was averaged over the whole exposure period ($n = 72$) and oxygen consumption rate (H) was measured after 77 days of exposure. ‘Subtidal’ and ‘Intertidal’ indicate the tidal treatment in which the oysters were placed (subtidal: constant immersion; intertidal: 8.5 h immersion and 3.5 h emersion). Data correspond to means \pm s.e.m. ($n = 3$ tanks). Different letters represent significant differences ($P < 0.05$) between conditions.

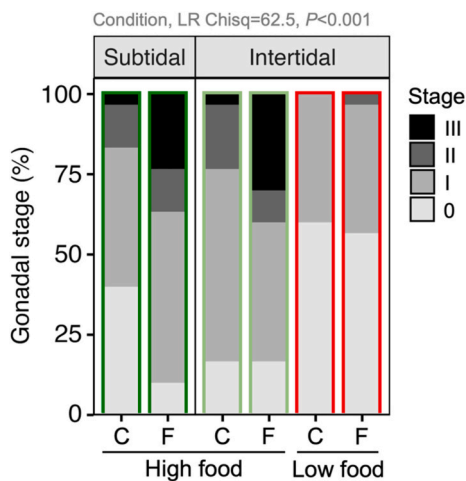


Fig. 3. Relative percentage of *Crassostrea gigas* oysters at each gonadal stage under different temperature and pH conditions, tidal treatment and food level at the end of the 81-day exposure period. Gonadal development was evaluated over 30 individuals per condition ($n = 10$ per tank). ‘Subtidal’ and ‘Intertidal’ indicate the tidal treatment in which the oysters were placed (subtidal: constant immersion; intertidal: 8.5 h immersion and 3.5 h emersion). Green boxes indicate high-fed oysters, while red boxes indicate low-fed oysters. C, current temperature and pH conditions; F, future temperature and pH conditions; Stage 0, inactive/resting stage; Stage I, early maturation; Stage II, advanced maturation; Stage III, mature animal with ripe or spawning gonad. (For interpretation of the references to colour in this figure legend, the reader is referred to the web version of this article.)

rate was higher under future OAW than under current conditions when oysters were permanently immersed (Fig. 2G; Table S1). In contrast, when oysters were regularly exposed to air, ingestion rate was not influenced by future OAW. Overall, the ingestion rate was higher in intertidal conditions than in subtidal conditions. The ingestion rate reported over a day, which considers the time during which the oysters were out of the water and not feeding, was similar between tidal conditions (Fig. S1).

3.2. Food availability is a major factor influencing oyster metabolism

The differences in growth-related parameters observed between current and future conditions faded under food limitation, and overall, oysters exhibited lower growth rates under such nutritional conditions (Fig. 2A-F; Table S1). This interactive effect between temperature/pH conditions and food level was clearly reflected in the gonadal

development of oysters, as ~25 % of oysters reared under future conditions with high food level were fully mature (stage III), compared to only 3 % under current conditions with high food, and 0 % under low food conditions regardless of temperature/pH conditions (Fig. 3). In fact, most of the oysters maintained under low feeding conditions had immature gonads (on average 58 % were at stage 0) or showed early gonadal development (stage I). Ingestion rate of oysters under high food conditions was about twice that of oysters under limited food, and there was no effect of temperature/pH conditions (Fig. 2G; Table S1). In addition, oxygen consumption rates of oysters were about 2-fold higher under low food conditions (Fig. 2H; Table S1).

3.3. Food is the main driver of energy reserves in oysters

We found that the lipid reserves, evaluated using the TAG:ST ratio, and the carbohydrate content of oysters were respectively nearly 2- and 3-fold higher under high food level compared to those maintained under food limitation, regardless of the temperature/pH conditions and tidal treatment (Fig. 4; Table S1). Protein content was much less variable than TAG:ST ratio and carbohydrates, and the lowest level was recorded in oysters maintained under future, intertidal and low food conditions.

3.4. All tested factors modulate membrane fatty acids

The major fatty acids - those that represent more than 5 % of the polar fatty acids - found in oyster tissues were eicosapentaenoic acid (EPA, 20:5n-3, 16.8 %), palmitic acid (16:0, 16.0 %), stearic acid (18:0, 7.2 %), docosahexaenoic acid (DHA, 22:6n-3, 7.1 %), vaccenic acid (18:1n-7, 6.8 %), and the non-methylene-interrupted fatty acids (22:2NMI, 5.5 %). They together accounted for 59 % of polar fatty acids (Table S2). Multivariate analysis showed clear separation of membrane fatty acids depending on temperature/pH conditions, tidal treatment and food level (Fig. 5A; PERMANOVA, Condition, $R^2 = 0.75$, $F = 7.3$, $P < 0.001$). The unsaturation index of membrane fatty acids, an indicator of membrane fluidity, decreased under future conditions compared to current conditions (planned contrast between group means: future vs. current, estimate = 15.0 ± 3.8 , $Z = 3.9$, $P < 0.001$; Fig. 5B). This change in unsaturation index mainly reflected 20:5n-3 (future vs. current, estimate = 2.6 ± 0.5 , $Z = 5.1$, $P < 0.001$; Fig. 5E), 22:2NMI (future vs. current, estimate = 0.6 ± 0.2 , $Z = 2.5$, $P = 0.025$; Fig. 5F), but less 22:6n-3 (future vs. current, estimate = 0.5 ± 0.3 , $Z = 1.6$, $P = 0.219$; Fig. 5D). Arachidonic acid (20:4n-6), a fatty acid previously associated with stress response in bivalves, was minor, representing on average 0.9 % of polar fatty acids, and unaffected by temperature/pH conditions, tidal treatment and food level (Fig. 5C).

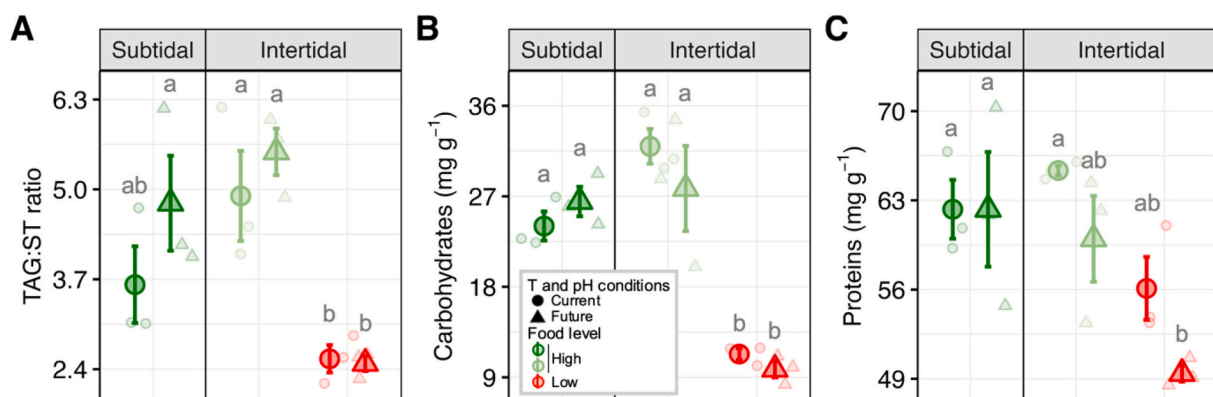


Fig. 4. Triacylglycerol:sterol ratio (A), total carbohydrate content (B) and total protein content (C) in *Crassostrea gigas* oysters under different temperature and pH conditions, tidal treatment and food level at the end of the 81-day exposure period, prior to viral challenge. ‘Subtidal’ and ‘Intertidal’ indicate the tidal treatment in which the oysters were placed (subtidal: constant immersion; intertidal: 8.5 h immersion and 3.5 h emersion). Data correspond to means \pm s.e.m. ($n = 3$ tanks). Different letters represent significant differences ($P < 0.05$) between conditions.

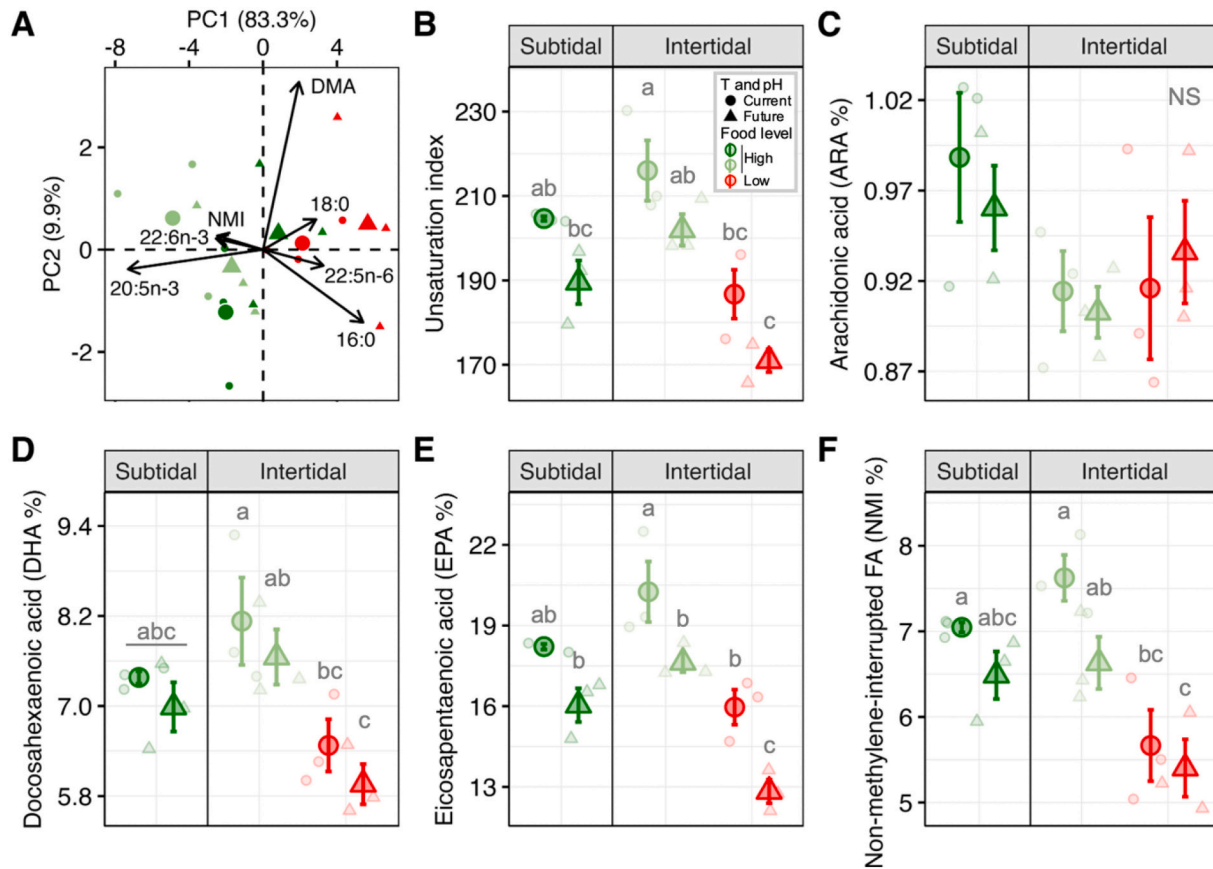


Fig. 5. Principal component analysis of polar fatty acids (A), unsaturation index (B), arachidonic acid (C), docosahexaenoic acid (D), eicosapentaenoic acid (E) and non-methylene-interrupted FA (F) in *Crassostrea gigas* oysters under different temperature and pH conditions, tidal treatment and food level at the end of the 81-day exposure period, prior to viral challenge. Arrows on principal component analysis (plot A) represent the average of the three replicates per condition. ‘Subtidal’ (in dark green) and ‘Intertidal’ (in light green and red) indicate the tidal treatment in which the oysters were placed (subtidal: constant immersion; intertidal: 8.5 h immersion and 3.5 h emersion). Data correspond to means ± s.e.m. ($n = 3$ tanks). Different letters represent significant differences ($P < 0.05$) between conditions. NS, non-significant difference. (For interpretation of the references to colour in this figure legend, the reader is referred to the web version of this article.)

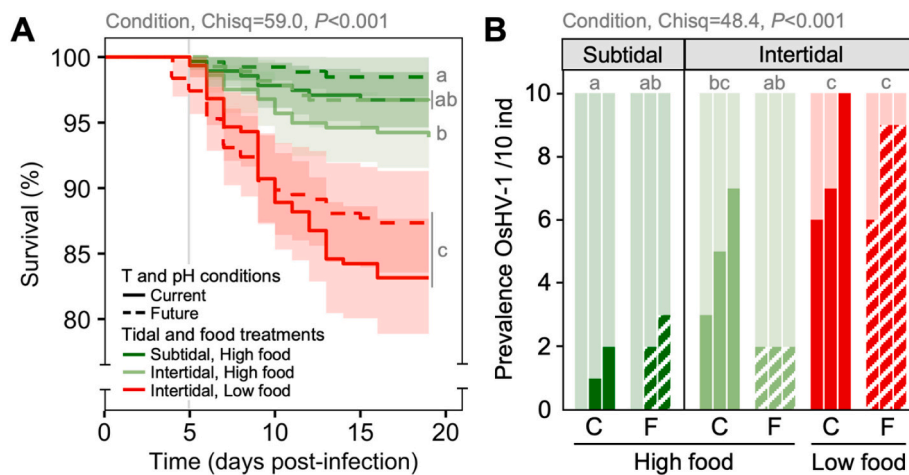


Fig. 6. Survival of *Crassostrea gigas* oysters challenged with OsHV-1 after exposure to different temperature and pH conditions, tidal treatments and food levels (A), and OsHV-1 prevalence in oysters after 5 days post-infection (dpi) (B). The thick lines in plot A represent average survival in each condition, while the vertical line indicates the animal sampling at 5 dpi for OsHV-1 prevalence analysis. The y-axis of plot B is the number of OsHV-1-positive oysters out of 10 tested for each tank and condition. There are three bars per condition, each corresponding to one tank (replicate). The darker lower part of the bars corresponds to positive individuals, while the lighter upper part corresponds to virus-negative individuals. Different letters represent significant differences ($P < 0.05$) between conditions. C, current temperature and pH conditions; F, future temperature and pH conditions.

3.5. Only food availability influences the susceptibility of oysters to disease

Pathogenic challenge induced moderate mortalities as survival were between $83.2 \pm 2.2\%$ for oysters under current, intertidal and low food conditions, and $98.5 \pm 0.8\%$ for those maintained under future, subtidal and high food conditions (Fig. 6A). On average, food limitation increased the risk of oyster mortality by 4.8 times compared to that under high food (Table 2). The risk of oyster mortality was unaffected by temperature/pH conditions (future vs. current, estimate = 0.5 ± 0.3 , $Z = 2.1$, $P = 0.067$) and tidal treatment (intertidal vs. subtidal, estimate = -0.8 ± 0.4 , $Z = -2.1$, $P = 0.068$).

Oyster mortalities were clearly associated with the detection of OsHV-1 DNA. The viral DNA was indeed detected in large quantities in dead oysters ($5.3 \cdot 10^5 \pm 6.9 \cdot 10^5$ OsHV-1 DNA cp mg⁻¹). Moreover, detection of viral DNA in live oysters sampled at 5 dpi varied among conditions, consistently with mortality risk (Fig. 6B). Virus prevalence was higher in low-fed oysters which had a higher risk of mortality than in high-fed oysters which had a lower risk of mortality (more than 22 vs. less than 7 positive individuals out of 30, respectively). These differences in survival and OsHV-1 prevalence in oysters among conditions were consistent with viral load (Table S3).

4. Discussion

We found that oysters are tolerant to ocean acidification and warming (OAW; +3 °C and -0.3 pH units) exhibiting phenotypic plasticity in physiological and biochemical traits. Indeed, future OAW increases oyster growth and reproduction when food is non-limiting. It is likely that this rise in temperature completely overrides the potential effects of acidification, and that future OAW conditions are still within the tolerance range of *C. gigas*. Concomitantly, the lack of food clearly negates the beneficial effect of OAW through an antagonistic interaction, as energy intake is not sufficient to enable stronger growth. Also, the susceptibility to viral disease of oysters was unaffected by future temperature/pH conditions, suggesting that acclimation to OAW does not induce physiological trade-offs between immunity and other fitness-related functions. Conversely, disease susceptibility increased in low-fed oysters. All these observations suggest that food availability is the predominant factor influencing the physiological responses of oysters to OAW and disease susceptibility. Finally, the tidal treatment had no major effect on the physiological performance of the oysters, as they are fully adapted to compensate for lower amount of time when phytoplankton is available.

4.1. Oysters are robust to ocean acidification and warming

We found that when food is non-limiting, oysters grow and reproduce faster under future OAW conditions than under current conditions, probably reflecting the dominating effect of warming over acidification. Since the experimental design considers a combined treatment of high temperature and low pH, it is impossible to know the individual effect of

Table 2

Summary of mixed-effects Cox model for survival to OsHV-1 of *Crassostrea gigas* oysters previously exposed to different temperature and pH conditions, tidal treatment and food level. Reference condition was 'Current T and pH conditions x Subtidal treatment x High food level'. Significant *P*-values ($P < 0.05$) are indicated in bold.

Condition	Estimate	SE	Z	P	Odds ratio
Future, Subtidal, HF	-0.79	0.60	-1.31	0.19	0.45
Current, Intertidal, HF	0.64	0.41	1.55	0.12	1.89
Future, Intertidal, HF	0.10	0.46	0.21	0.83	1.10
Current, Intertidal, LF	1.69	0.36	4.65	<0.001	5.44
Future, Intertidal, LF	1.43	0.37	3.82	<0.001	4.16

HF, high food; LF, low food.

either based on the present results. In ectothermic organisms like oysters, warming accelerates the velocity of chemical reactions, metabolic rates and overall development (Hochachka and Somero, 2002). Although decreasing pH can reduce net calcification and shell growth of oysters (Gazeau et al., 2013; Ries et al., 2009; Ross et al., 2024), this effect can be compensated by warming which accelerates the metabolism. Studies conducted on Pacific oyster and sea urchin have also reported that warming can mitigate the impacts of reduced pH, even resulting in greater growth under OAW than under control conditions (Dworjanyn and Byrne, 2018; Ko et al., 2014). In addition, sexual ripeness of Pacific oysters is reached earlier under OAW conditions, as already observed in a similar study (Di Poi et al., 2022). It is also possible that the decrease of 0.3 pH units applied in our study has no effect if it is still within the tolerance range of *C. gigas* (Lutier et al., 2022). Overall, oysters thrived under OAW, as these conditions are likely within their optimal performance range, coupled with the fact that oysters had high energy intakes through ad libitum feeding.

In contrast to previous studies, warming and acidification did not affect disease susceptibility of oysters (Ellis et al., 2015; Matozzo et al., 2012). The increased growth of oysters at 23 °C compared to those maintained at 20 °C could have favored virus replication and associated mortalities, which depend directly on host metabolism (Petton et al., 2023). In addition, lower pH has already been identified as a factor aggravating virus-induced oyster mortalities (Fuhrmann et al., 2019), whereas this is not the case in our study under future OAW conditions. The lack of effects is likely due to the relatively low mortalities observed after exposure to the virus, which consequently limits the expression of variance. Nevertheless, the fact that oyster susceptibility to disease is not increased under future OAW experimental conditions suggests that there are no additional physiological costs requiring trade-offs between immunity and other functions.

Although our data suggest that the highly-fed oysters under future OAW were maintained in low-stress conditions, they nevertheless showed plastic phenotypic responses: accelerated growth and reproduction supported by increased food consumption in the case of subtidal oysters. Another striking evidence of the acclimation response to the future OAW conditions is the major remodeling of membrane lipids. We indeed found that the unsaturation index of fatty acids (FA), an indicator of the membrane fluidity, was lower under future OAW conditions than under current conditions, due to lower levels of polyunsaturated FA (PUFA) such as EPA (20:5n-3) and non-methylene-interrupted FA (22:2NMI). These changes are consistent with the homeoviscous adaptation theory (Hazel, 1995), which suggests that increasing temperature increases the fluidity and disorder in ectotherms' cell membranes, potentially leading to significant metabolic dysfunctions. Consequently, ectotherms adjust the unsaturation level of membrane FA to counteract temperature-induced changes in membrane fluidity, based on the principle that the higher the level of unsaturation, the more fluid the membranes. The homeoviscous response via the regulation of membrane PUFAs, including 20:5n-3 and NMI, has already been reported in several bivalve species such as oysters, mussels and clams from different thermal habitats (Le Luyer et al., 2022 and references therein; Pernet et al., 2007). In addition, just like increasing temperature, decreasing pH reduces membrane PUFAs in oysters but the causes remain to be elucidated (Caillon et al., 2023; Di Poi et al., 2022; Lutier et al., 2022). Therefore, membrane plasticity is also a key parameter that may help oysters acclimatize to acidification and warming.

4.2. Food availability is the main driver affecting responses of oysters to OAW and disease susceptibility

The increase in food availability accelerated the growth and reproduction of oysters in interaction with the OAW scenario. Under low food and future OAW conditions, oysters did not exhibit the increase in growth and reproduction observed when highly fed, suggesting an antagonistic interaction. Therefore, food can act as a limiting factor in

the response of organisms to environmental drivers, meaning that energy intake from low food supply and ingestion rate may not be sufficient to sustain higher metabolic rates under the future OAW conditions. Likewise, the growth of juvenile sea bass (*Dicentrarchus labrax*) and cold-water coral (*Lophelia pertusa*) did not differ between individuals reared under ambient and future OAW conditions when food was limiting (Büscher et al., 2017; Cominassi et al., 2020). We therefore highlight the importance of incorporating realistic food levels into experimental designs examining OAW. Ad libitum feeding, used in the majority of studies to date, may have minimized impacts, or conversely overestimated them if animals were not fed (Cominassi et al., 2020; Ramajo et al., 2016).

Low food condition increases mortality and infection in oysters during virus challenge, irrespective of temperature and pH conditions and tidal treatment. The relationship between food level and disease susceptibility is complex because a low quantity of food can reduce the host's physiological condition, thereby increasing its susceptibility to infectious diseases. Yet, food limitation can also slow down the growth and metabolism of the host, which the pathogen relies on for its own proliferation (Civitello et al., 2018; Smith et al., 2005). This illustrates a delicate balance between immunity and other fitness-related functions (Lochmiller and Deerenberg, 2000). Regarding oysters and OsHV-1, short-lasting dietary restrictions generally lead to a reduction in disease susceptibility in oysters exposed to OsHV-1 (Evans et al., 2015; Moreau et al., 2015; Pernet et al., 2019b; Petton et al., 2023). Although this seems contradictory to our results, the effect of food limitation on disease susceptibility may change depending on intensity and duration. When subjected to prolonged dietary restriction, as observed in the current study over a period of three months, oysters experienced a significant depletion in lipid and carbohydrate reserves, but also in proteins which are generally used as a last resort (Aldridge et al., 1995; Pörtner et al., 1999). This reduction in available energy has likely permanently weakened the metabolism and immune defenses of oysters, overshadowing the positive effect of reduced host metabolism on viral proliferation and mortality.

Concomitantly, our results on the aerobic performance of oysters suggest increased sensitivity of oysters under low food conditions. Indeed, we observed that the oxygen consumption rate, a proxy for metabolic rates, increased in low-fed oysters. In aquatic ectotherms, an increase in the standard metabolic rate indicates a shift into the species' pejus state and that more energy is required for basal maintenance (Sokolova, 2021; Sokolova et al., 2012). This implies that a lack of food can disrupt the energy budget and physiological trade-offs of oysters, especially when they are exposed to other environmental constraints. In contrast, OAW had no impact on the metabolic rates of oysters, indicating no increase in energy demand. Oysters can therefore tolerate ocean acidification and warming, but perhaps not in a state of nutritional deficiency.

4.3. Effect of tidal treatment does not interact with ocean acidification and warming, reflecting compensatory mechanism

We did not identify any significant effect of tidal exposure on macrophysiological traits such as growth, reproduction, respiration, and survival to pathogen exposure, despite intertidal oysters being surrounded by food and pathogens for less time than their subtidal counterparts. Field studies on Pacific oysters have shown that tidal height is associated with slower oyster growth and a lower risk of mortality (Azéma et al., 2017; Bordignon et al., 2020; Pernet et al., 2019a). In contrast, Wallès et al. (2016) reported that oyster growth and recruitment are optimal around 20 to 40 %, following a unimodal curve. Due to the different study systems, we can expect differences from field studies, where several other environmental factors are involved. Our results suggest that physiological compensatory mechanisms may occur during emersion. We indeed observed that intertidal oysters ingest more food per unit of available time for feeding, thereby compensating for the food

limitations imposed by air exposure (Gillmor, 1982). The fact that both subtidal and intertidal oysters ingest the same amount of food over a day, considering emersion time, explains the identical growth rates observed between the two groups. Also, the beneficial effects of OAW are observed similarly in both intertidal and subtidal conditions, indicating no synergistic or antagonistic effect with tidal treatment.

Our results contrast with those of Scanes et al. (2017) on adults of the Sydney rock oyster *Saccostrea glomerata*, who found that OA and tidal emersion have synergistic and sublethal effects as oysters reach their physiological limit of tolerance to hypercapnia. Beyond possible species-related effects, discrepancies between studies possibly reflect differences in duration of air exposure (emersion time was 75 % in Scanes et al. (2017) compared to 30 % here). For instance, hypercapnia during emersion caused a drop in extracellular pH of 0.6 pH units that was not fully compensated by the end of the immersion cycle of *S. glomerata* (Scanes et al., 2017). We did not measure the internal pH of the oysters, so we cannot make a direct comparison. However, the fact that there is no effect on growth suggests that this drop in internal pH is small or that growth during immersion compensates for it.

Interestingly, we found that the shell length of intertidal oysters under the future OAW scenario is comparable to that of their subtidal counterparts, but their shell weight was reduced, suggesting alterations in shell thickness and/or density. This could be explained by the dissolution of the shell during emersion to release bicarbonate ions (HCO_3^-) in order to compensate for internal acidosis and extracellular acid-base disturbances (Michaelidis et al., 2005; Scanes et al., 2017). Overall, further investigation into the structural and mechanical properties of the shells is required to fully understand the potential combined effects of emersion and future seawater conditions on calcification.

4.4. Conclusion

In this study, we attempted to more closely mimic the natural environment of oysters in the laboratory to better assess the impact of OAW, while accounting for drivers such as tidal treatment and food availability. Although tidal exposure did not have a major influence on oyster responses to OAW, it is important to continue considering the effects of this factor on intertidal organisms for ecological realism. In scenarios with even more pronounced OAW, air exposure could become a limiting factor in the acclimation response. Therefore, it would be valuable to investigate a performance curve for intertidal organisms in relation to OAW, considering the variable of air exposure.

A significant finding from this study is the paramount influence of food availability on the acclimation response of oysters to OAW, as well as their susceptibility to disease. While OAW is expected to increase the metabolism and nutritional demands of marine organisms (Clements and Darrow, 2018), it is also likely to coincide with a decline in primary production due to increased ocean stratification and severe droughts, which limit nutrient supply and availability (Behrenfeld et al., 2006; Wetz et al., 2011). Consequently, OAW may exacerbate the challenge of aligning food supply with the nutritional needs of organisms. In the natural environment, oysters are additionally exposed to other dynamic and interconnected factors, such as salinity regimes and dissolved oxygen, which further impact their growth and challenge their energy demands. These misalignments could lead to trophic mismatches, ultimately jeopardizing both natural oyster populations and the shellfish industry.

CRedit authorship contribution statement

Coline Caillon: Writing – review & editing, Writing – original draft, Visualization, Validation, Methodology, Investigation, Formal analysis, Data curation, Conceptualization. **Elodie Fleury:** Writing – review & editing, Visualization, Supervision, Resources, Methodology, Investigation, Funding acquisition, Conceptualization. **Carole Di Poi:** Writing – review & editing, Visualization, Investigation. **Frédéric Gazeau:**

Writing – review & editing, Visualization, Investigation. **Fabrice Pernet**: Writing – review & editing, Writing – original draft, Validation, Supervision, Project administration, Methodology, Investigation, Funding acquisition, Formal analysis, Conceptualization.

Funding

The study was supported by the ECOSCOPA network (Convention DPMA 2021) and the CocoriCO₂ project funded by the European Maritime and Fisheries Fund (EMFF, grant no. 344, 2020–2023).

Declaration of competing interest

The authors declare that they have no known competing financial interests or personal relationships that could have appeared to influence the work reported in this paper.

Acknowledgements

This work is part of the PhD thesis of Coline Caillon (Caillon, 2023). We are particularly grateful to Moussa Diagne for phytoplankton production, Lucie Chauvel, Edgar Caput, Matthias Huber, Hugo Koechlin, Théo Gromberg, Jacqueline Le Grand and Isabelle Queau for zootechnical support, Valérian Le Roy and Claudie Quéré for biochemical analyses, Christine Dubreuil for molecular analyses, Virgile Quillien for histological analyses, Elodie Foucault and Vincent Ouisse for total alkalinity analyses, Benjamin Morga for providing the viral suspension, and José-Luis Zambonino-Infante for commenting on the final manuscript.

Appendix A. Supplementary data

Supplementary data to this article can be found online at <https://doi.org/10.1016/j.aquaculture.2025.742459>.

Data availability

The data supporting the findings of this study are openly available at the SEANO data repository: <https://doi.org/10.17882/102048>.

References

Aldridge, D.W., Payne, B.S., Miller, A.C., 1995. Oxygen consumption, nitrogenous excretion, and filtration rates of *Dreissena polymorpha* at acclimation temperatures between 20 and 32 °C. *Can. J. Fish. Aquat. Sci.* 52, 1761–1767. <https://doi.org/10.1139/f95-768>.

Andreyeva, A.Y., Kukhareva, T.A., Gostyukhina, O.L., Vialova, O.Y., Tkachuk, A.A., Chelebueva, E.S., Podolskaya, M.S., Borovkov, A.B., Bogacheva, E.A., Lavrichenko, D. S., Kladchenko, E.S., 2024. Impacts of ocean acidification and hypoxia on cellular immunity, oxygen consumption and antioxidant status in Mediterranean mussel. *Fish Shellfish Immunol.* 154, 109932. <https://doi.org/10.1016/j.fsi.2024.109932>.

Azéma, P., Maurouard, E., Lamy, J.-B., Dégremont, L., 2017. The use of size and growing height to improve *Crassostrea gigas* farming and breeding techniques against OsHV-1. *Aquaculture* 471, 121–129. <https://doi.org/10.1016/j.aquaculture.2017.01.011>.

Barbosa Solomieu, V., Renault, T., Travers, M.-A., 2015. Mass mortality in bivalves and the intricate case of the Pacific oyster, *Crassostrea gigas*. *J. Invertebr. Pathol.* 131, 2–10. <https://doi.org/10.1016/j.jip.2015.07.011>.

Bayne, B.L., 2017. *Biology of Oysters*. Academic Press.

Behrenfeld, M.J., O'Malley, R.T., Siegel, D.A., McClain, C.R., Sarmiento, J.L., Feldman, G.C., Milligan, A.J., Falkowski, P.G., Letelier, R.M., Boss, E.S., 2006. Climate-driven trends in contemporary ocean productivity. *Nature* 444, 752–755. <https://doi.org/10.1038/nature05317>.

Bibby, R., Widdicombe, S., Parry, H., Spicer, J., Pipe, R., 2008. Effects of ocean acidification on the immune response of the blue mussel *Mytilus edulis*. *Aquat. Biol.* 2, 67–74. <https://doi.org/10.1038/ab00037>.

Bordignon, F., Zomeño, C., Xiccato, G., Birolo, M., Pascual, A., Trocino, A., 2020. Effect of emersion time on growth, mortality and quality of Pacific oysters (*Crassostrea gigas*, Thunberg 1973) reared in a suspended system in a lagoon in Northern Italy. *Aquaculture* 528, 735481. <https://doi.org/10.1016/j.aquaculture.2020.735481>.

Bougrier, S., Geairon, P., Deslous-Paoli, J.M., Bacher, C., Jonquière, G., 1995. Allometric relationships and effects of temperature on clearance and oxygen consumption rates of *Crassostrea gigas* (Thunberg). *Aquaculture* 134, 143–154. [https://doi.org/10.1016/0044-8486\(95\)00036-2](https://doi.org/10.1016/0044-8486(95)00036-2).

Boyd, P.W., Collins, S., Dupont, S., Fabricius, K., Gattuso, J.-P., Havenhand, J., Hutchins, D.A., Riebesell, U., Rintoul, M.S., Vichi, M., Biswas, H., Ciotti, A., Gao, K., Gehlen, M., Hurd, C.L., Kurihara, H., McGraw, C.M., Navarro, J.M., Nilsson, G.E., Passow, U., Pörtner, H.-O., 2018. Experimental strategies to assess the biological ramifications of multiple drivers of global ocean change—a review. *Glob. Chang. Biol.* 24, 2239–2261. <https://doi.org/10.1111/gcb.14102>.

Brown, N.E.M., Bernhardt, J.R., Anderson, K.M., Harley, C.D.G., 2018. Increased food supply mitigates ocean acidification effects on calcification but exacerbates effects on growth. *Sci. Rep.* 8, 1–9. <https://doi.org/10.1038/s41598-018-28012-w>.

Burnett, L.E., 1988. Physiological responses to air exposure: acid-base balance and the role of branchial water stores. *Am. Zool.* 28, 125–135. <https://doi.org/10.1093/icb/28.1.125>.

Büscher, J.V., Form, A.U., Riebesell, U., 2017. Interactive effects of ocean acidification and warming on growth, fitness and survival of the cold-water coral *Lophelia pertusa* under different food availabilities. *Front. Mar. Sci.* 4. <https://doi.org/10.3389/fmars.2017.00101>.

Byrne, M., Przeslawski, R., 2013. Multistressor impacts of warming and acidification of the ocean on marine invertebrates' life histories. *Integr. Comp. Biol.* 53, 582–596. <https://doi.org/10.1093/icb/ict049>.

Caillon, C., 2023. *Plasticité phénotypique des huîtres face à l'acidification et au réchauffement des océans sous différentes contraintes environnementales*. PhD thesis, Université de Bretagne occidentale.

Caillon, C., Pernet, F., Lutier, M., Di Poi, C., 2023. Differential reaction norms to ocean acidification in two oyster species from contrasting habitats. *J. Exp. Biol.* 226, jeb246432. <https://doi.org/10.1242/jeb.246432>.

Caldeira, K., Wickett, M.E., 2003. Anthropogenic carbon and ocean pH. *Nature* 425, 365. <https://doi.org/10.1038/425365a>.

Civitello, D.J., Fatima, H., Johnson, L.R., Nisbet, R.M., Rohr, J.R., 2018. Bioenergetic theory predicts infection dynamics of human schistosomes in intermediate host snails across ecological gradients. *Ecol. Lett.* 21, 692–701. <https://doi.org/10.1111/ele.12937>.

Clements, J.C., Darrow, E.S., 2018. Eating in an acidifying ocean: a quantitative review of elevated CO₂ effects on the feeding rates of calcifying marine invertebrates. *Hydrobiologia* 820, 1–21. <https://doi.org/10.1007/s10750-018-3665-1>.

Cole, V.J., Parker, L.M., O'Connor, S.J., O'Connor, W.A., Scanes, E., Byrne, M., Ross, P. M., 2016. Effects of multiple climate change stressors: ocean acidification interacts with warming, hyposalinity, and low food supply on the larvae of the brooding flat oyster *Ostrea angasi*. *Mar. Biol.* 163, 125. <https://doi.org/10.1007/s00227-016-2880-4>.

Cominassi, L., Moyano, M., Claireaux, G., Howald, S., Mark, F.C., Zambonino-Infante, J.-L., Peck, M.A., 2020. Food availability modulates the combined effects of ocean acidification and warming on fish growth. *Sci. Rep.* 10, 2338. <https://doi.org/10.1038/s41598-020-58846-2>.

Couturier, L.L.E., Michel, L.N., Amaro, T., Budge, S.M., da Costa, E., De Troch, M., Di Dato, V., Fink, P., Giraldo, C., Le Grand, F., Loaiza, I., Mathieu-Roudant, M., Nichols, P.D., Parrish, C.C., Sardenne, F., Vagner, M., Pernet, F., Soude, P., 2020. State of art and best practices for fatty acid analysis in aquatic sciences. *ICES J. Mar. Sci.* 77, 2375–2395. <https://doi.org/10.1093/icesjms/fsaa121>.

Di Poi, C., Brodu, N., Gazeau, F., Pernet, F., 2022. Life-history traits in the Pacific oyster *Crassostrea gigas* are robust to ocean acidification under two thermal regimes. *ICES J. Mar. Sci.* 79, 2614–2629. <https://doi.org/10.1093/icesjms/fsac195>.

Dickson, A.G., Sabine, C.L., Christian, J.R., Barger, C.P., North Pacific Marine Science Organization (Eds.), 2007. *Guide to Best Practices for Ocean CO₂ Measurements*, PICES Special Publication. North Pacific Marine Science Organization, Sidney, BC.

Dubois, Michel, Gilles, K.A., Hamilton, J.K., Rebers, P.A., Smith, Fred, 1956. Colorimetric method for determination of sugars and related substances. *Anal. Chem.* 28, 350–356. <https://doi.org/10.1021/ac60111a017>.

Dugeny, E., de Lorigeril, J., Petton, B., Toulza, E., Gueguen, Y., Pernet, F., 2022. Seaweeds influence oyster microbiota and disease susceptibility. *J. Anim. Ecol.* 91, 805–818. <https://doi.org/10.1111/1365-2656.13662>.

Dworjanyn, S.A., Byrne, M., 2018. Impacts of ocean acidification on sea urchin growth across the juvenile to mature adult life-stage transition is mitigated by warming. *Proc. R. Soc. B Biol. Sci.* 285, 20172684. <https://doi.org/10.1098/rspb.2017.2684>.

EFSA Panel on Animal Health and Welfare (AHAW), 2015. Oyster mortality. *EFSA J.* 13, 4122. <https://doi.org/10.2903/j.efsa.2015.4122>.

Ellis, R.P., Widdicombe, S., Parry, H., Hutchinson, T.H., Spicer, J.I., 2015. Pathogenic challenge reveals immune trade-off in mussels exposed to reduced seawater pH and increased temperature. *J. Exp. Mar. Biol. Ecol.* 462, 83–89. <https://doi.org/10.1016/j.jembe.2014.10.015>.

Evans, O., Hick, P., Dhand, N., Whittington, R.J., 2015. Transmission of Ostreid herpesvirus-1 in *Crassostrea gigas* by cohabitation: effects of food and number of infected donor oysters. *Aquac. Environ. Interact.* 7, 281–295. <https://doi.org/10.3354/aei00160>.

Fabioux, C., Huvet, A., Le Souchu, P., Le Pennec, M., Pouvreau, S., 2005. Temperature and photoperiod drive *Crassostrea gigas* reproductive internal clock. *Aquaculture* 250, 458–470. <https://doi.org/10.1016/j.aquaculture.2005.02.038>.

Fu, W., Randerson, J.T., Moore, J.K., 2016. Climate change impacts on net primary production (NPP) and export production (EP) regulated by increasing stratification and phytoplankton community structure in the CMIP5 models. *Biogeosciences* 13, 5151–5170. <https://doi.org/10.5194/bg-13-5151-2016>.

Fuhrmann, M., Richard, G., Quéré, C., Petton, B., Pernet, F., 2019. Low pH reduced survival of the oyster *Crassostrea gigas* exposed to the Ostreid herpesvirus 1 by altering the metabolic response of the host. *Aquaculture* 503, 167–174. <https://doi.org/10.1016/j.aquaculture.2018.12.052>.

- Gazeau, F., Parker, L.M., Comeau, S., Gattuso, J.-P., O'Connor, W.A., Martin, S., Pörtner, H.-O., Ross, P.M., 2013. Impacts of ocean acidification on marine shelled molluscs. *Mar. Biol.* 160, 2207–2245. <https://doi.org/10.1007/s00227-013-2219-3>.
- Gillmore, R.B., 1982. Assessment of intertidal growth and capacity adaptations in suspension-feeding bivalves. *Mar. Biol.* 68, 277–286. <https://doi.org/10.1007/BF00409594>.
- Hazel, J.R., 1995. Thermal adaptation in biological membranes: is homeoviscous adaptation the explanation? *Annu. Rev. Physiol.* 57, 19–42. <https://doi.org/10.1146/annurev.ph.57.030195.000315>.
- Helmuth, B., Mieszkowska, N., Moore, P., Hawkins, S.J., 2006. Living on the edge of two changing worlds: forecasting the responses of rocky intertidal ecosystems to climate change. *Annu. Rev. Ecol. Syst.* 37, 373–404. <https://doi.org/10.1146/annurev.ecolsys.37.091305.110149>.
- Hettinger, A., Sanford, E., Hill, T.M., Hosfelt, J.D., Russell, A.D., Gaylord, B., 2013. The influence of food supply on the response of Olympia oyster larvae to ocean acidification. *Biogeosciences* 10, 6629–6638. <https://doi.org/10.5194/bg-10-6629-2013>.
- Hochachka, P.W., Somero, G.N., 2002. *Biochemical Adaptation: Mechanism and Process in Physiological Evolution*. Oxford University Press.
- Hulbert, A.J., Pamplona, R., Buffenstein, R., Butte, W.A., 2007. Life and death: metabolic rate, membrane composition, and life span of animals. *Physiol. Rev.* 87, 1175–1213. <https://doi.org/10.1152/physrev.00047.2006>.
- IPCC, 2022. In: Pörtner, H.-O., Roberts, D.C., Tignor, M., Poloczanska, E.S., Mintenbeck, K., Alegria, A., Craig, M., Langsdorf, S., Löschke, S., Möller, V., Okem, A., Rama, B. (Eds.), *Climate Change 2022: Impacts, Adaptation and Vulnerability*. Contribution of Working Group II to the Sixth Assessment Report of the Intergovernmental Panel on Climate Change. Cambridge University Press. Cambridge University Press, Cambridge, UK and New York, NY, USA. <https://doi.org/10.1017/9781009325844>, 3056 pp.
- Ko, G.W.K., Dineshram, R., Campanati, C., Chan, V.B.S., Havenhand, J., Thiyyagarajan, V., 2014. Interactive effects of ocean acidification, elevated temperature, and reduced salinity on early-life stages of the Pacific oyster. *Environ. Sci. Technol.* 48, 10079–10088. <https://doi.org/10.1021/es501611u>.
- Kroeker, K.J., Kordas, R.L., Crim, R., Hendriks, I.E., Ramajo, L., Singh, G.S., Duarte, C.M., Gattuso, J.-P., 2013. Impacts of ocean acidification on marine organisms: quantifying sensitivities and interaction with warming. *Glob. Chang. Biol.* 19, 1884–1896. <https://doi.org/10.1111/gcb.12179>.
- Le Luyer, J., Monaco, C.J., Milhade, L., Reisser, C., Soye, C., Raapoto, H., Belliard, C., Le Moullac, G., Ky, C.-L., Pernet, F., 2022. Gene expression plasticity, genetic variation and fatty acid remodeling in divergent populations of a tropical bivalve species. *J. Anim. Ecol.* 91, 1196–1208. <https://doi.org/10.1111/1365-2656.13706>.
- Lefebvre, S., Hussenet, J., Bossard, N., 1996. Water treatment of land-based fish farm effluents by outdoor culture of marine diatoms. *J. Appl. Phycol.* 8, 193–200. <https://doi.org/10.1007/BF02184971>.
- Lochmiller, R.L., Deerenberg, C., 2000. Trade-offs in evolutionary immunology: just what is the cost of immunity? *Oikos* 88, 87–98. <https://doi.org/10.1034/j.1600-0706.2000.880110.x>.
- Lowry, O.H., Rosebrough, N.J., Farr, A.L., Randall, R.J., 1951. Protein measurement with the Folin phenol reagent. *J. Biol. Chem.* 193, 265–275. [https://doi.org/10.1016/S0021-9258\(19\)52451-6](https://doi.org/10.1016/S0021-9258(19)52451-6).
- Lutier, M., Di Poi, C., Gazeau, F., Appolis, A., Le Luyer, J., Pernet, F., 2022. Revisiting tolerance to ocean acidification: insights from a new framework combining physiological and molecular tipping points of Pacific oyster. *Glob. Chang. Biol.* 28, 3333–3348. <https://doi.org/10.1111/gcb.16101>.
- Martenot, C., Oden, E., Travaille, E., Malas, J.P., Houssin, M., 2010. Comparison of two real-time PCR methods for detection of ostreid herpesvirus 1 in the Pacific oyster *Crassostrea gigas*. *J. Virol. Methods* 170, 86–89. <https://doi.org/10.1016/j.jviromet.2010.09.003>.
- Matozzo, V., Chinellato, A., Munari, M., Finos, L., Bressan, M., Marin, M.G., 2012. First evidence of immunomodulation in bivalves under seawater acidification and increased temperature. *PLoS ONE* 7, e33820. <https://doi.org/10.1371/journal.pone.0033820>.
- Melzner, F., Stange, P., Trübenbach, K., Thomsen, J., Casties, I., Panknin, U., Gorb, S.N., Gutowska, M.A., 2011. Food supply and seawater pCO₂ impact calcification and internal shell dissolution in the blue mussel *Mytilus edulis*. *PLoS ONE* 6, e24223. <https://doi.org/10.1371/journal.pone.0024223>.
- Michaelidis, B., Haas, D., Grieshaber, M.K., 2005. Extracellular and intracellular acid-base status with regard to the energy metabolism in the oyster *Crassostrea gigas* during exposure to air. *Physiol. Biochem. Zool.* 78, 373–383. <https://doi.org/10.1086/430223>.
- Moreau, P., Moreau, K., Segarra, A., Tourbiez, D., Travers, M.-A., Rubinsztein, D.C., Renault, T., 2015. Autophagy plays an important role in protecting Pacific oysters from OsHV-1 and *vibrio aestuarianus* infections. *Autophagy* 11, 516–526. <https://doi.org/10.1080/15548627.2015.1017188>.
- O'Connor, W.A., Nell, J.A., Diemar, J.A., 1992. The evaluation of twelve algal species as food for juvenile Sydney rock oysters *Saccostrea commercialis* (Iredale & Roughley). *Aquaculture* 108, 277–283. [https://doi.org/10.1016/0044-8486\(92\)90112-X](https://doi.org/10.1016/0044-8486(92)90112-X).
- Orr, J.C., Fabry, V.J., Aumont, O., Bopp, L., Doney, S.C., Feely, R.A., Gnanadesikan, A., Gruber, N., Ishida, A., Joos, F., Key, R.M., Lindsay, K., Maier-Reimer, E., Matear, R., Monfray, P., Mouchet, A., Najjar, R.G., Plattner, G.-K., Rodgers, K.B., Sabine, C.L., Sarmiento, J.L., Schlitzer, R., Slater, R.D., Totterdell, L.J., Weirig, M.-F., Yamanaka, Y., Yool, A., 2005. Anthropogenic ocean acidification over the twenty-first century and its impact on calcifying organisms. *Nature* 437, 681–686. <https://doi.org/10.1038/nature04095>.
- Parker, L.M., O'Connor, W.A., Byrne, M., Coleman, R.A., Virtue, P., Dove, M., Gibbs, M., Spohr, L., Scanes, E., Ross, P.M., 2017. Adult exposure to ocean acidification is maladaptive for larvae of the Sydney rock oyster *Saccostrea glomerata* in the presence of multiple stressors. *Biol. Lett.* 13, 20160798. <https://doi.org/10.1098/rsbl.2016.0798>.
- Parker, L.M., Scanes, E., O'Connor, W.A., Ross, P.M., 2021. Transgenerational plasticity responses of oysters to ocean acidification differ with habitat. *J. Exp. Biol.* 224, jeb239269. <https://doi.org/10.1242/jeb.239269>.
- Pernet, F., Tremblay, R., Comeau, L., Guderley, H., 2007. Temperature adaptation in two bivalve species from different thermal habitats: energetics and remodeling of membrane lipids. *J. Exp. Biol.* 210, 2999–3014. <https://doi.org/10.1242/jeb.006007>.
- Pernet, F., Gachelin, S., Stanisière, J.-Y., Petton, B., Fleury, E., Mazurié, J., 2019a. Farmer monitoring reveals the effect of tidal height on mortality risk of oysters during a herpesvirus outbreak. *ICES J. Mar. Sci.* 76, 1816–1824. <https://doi.org/10.1093/icesjms/fsz074>.
- Pernet, F., Tamayo, D., Fuhrmann, M., Petton, B., 2019b. Deciphering the effect of food availability, growth and host condition on disease susceptibility in a marine invertebrate. *J. Exp. Biol.* jeb.210534. <https://doi.org/10.1242/jeb.210534>.
- Petton, B., Boudry, P., Alunno-Bruscia, M., Pernet, F., 2015. Factors influencing disease-induced mortality of Pacific oysters *Crassostrea gigas*. *Aquac. Environ. Interact.* 6, 205–222. <https://doi.org/10.3354/aei00125>.
- Petton, B., Alunno-Bruscia, M., Mitta, G., Pernet, F., 2023. Increased growth metabolism promotes viral infection in a susceptible oyster population. *Aquac. Environ. Interact.* 15, 19–33. <https://doi.org/10.3354/aei00450>.
- Petton, S., Pernet, F., Le Roy, V., Huber, M., Martin, S., Macé, É., Bozec, Y., Loisel, S., Rimmelin-Maury, P., Grossteffan, É., Repecaud, M., Quemener, L., Retho, M., Manac'h, S., Papin, M., Pineau, P., Lacoue-Labarthe, T., Deborde, J., Costes, L., Polsenaere, P., Rigouin, L., Benhamou, J., Gouriou, L., Lequeux, J., Labourdette, N., Savoye, N., Messiaen, G., Foucault, E., Ouisse, V., Richard, M., Lagarde, F., Voron, F., Kempf, V., Mas, S., Giannecchini, L., Vidussi, F., Mostajir, B., Leredde, Y., Alliouane, S., Gattuso, J.-P., Gazeau, F., 2024. French coastal network for carbonate system monitoring: the CocoriCO₂ dataset. *Earth Syst. Sci. Data* 16, 1667–1688. <https://doi.org/10.5194/essd-16-1667-2024>.
- Pörtner, H.-O., 2008. Ecosystem effects of ocean acidification in times of ocean warming: a physiologist's view. *Mar. Ecol. Prog. Ser.* 373, 203–217. <https://doi.org/10.3354/meps07768>.
- Pörtner, H.O., Peck, L., Zielinski, S., Conway, L.Z., 1999. Intracellular pH and energy metabolism in the highly stenothermal Antarctic bivalve *Limopsis marionensis* as a function of ambient temperature. *Polar Biol.* 22, 17–30. <https://doi.org/10.1007/s003000050386>.
- Ramajo, L., Pérez-León, E., Hendriks, I.E., Marbà, N., Krause-Jensen, D., Sejr, M.K., Blicher, M.E., Lagos, N.A., Olsen, Y.S., Duarte, C.M., 2016. Food supply confers calcifiers resistance to ocean acidification. *Sci. Rep.* 6, 19374. <https://doi.org/10.1038/srep19374>.
- Riebesell, U., Gattuso, J.-P., 2015. Lessons learned from ocean acidification research. *Nat. Clim. Chang.* 5, 12–14. <https://doi.org/10.1038/nclimate2456>.
- Ries, J.B., Cohen, A.L., McCorkle, D.C., 2009. Marine calcifiers exhibit mixed responses to CO₂-induced ocean acidification. *Geology* 37, 1131–1134. <https://doi.org/10.1130/G30210A.1>.
- Ross, P.M., Pine, C., Scanes, E., Byrne, M., O'Connor, W.A., Gibbs, M., Parker, L.M., 2024. Meta-analyses reveal climate change impacts on an ecologically and economically significant oyster in Australia. *iScience* 27. <https://doi.org/10.1016/j.isci.2024.110673>.
- Rowley, A.F., Baker-Austin, C., Boerlage, A.S., Caillon, C., Davies, C.E., Duperré, L., Martin, S.A.M., Mitta, G., Pernet, F., Pratoomyot, J., Shields, J.D., Shinn, A.P., Songsunthong, W., Srijuntongsiri, G., Sritunyaluckana, K., Vidal-Dupiol, J., Webster, T.M.U., Taengchaiyaphum, S., Wongwaradechkul, R., Coates, C.J., 2024. Diseases of marine fish and shellfish in an age of rapid climate change. *iScience* 27. <https://doi.org/10.1016/j.isci.2024.110838>.
- Scanes, E., Parker, L.M., O'Connor, W.A., Stapp, L.S., Ross, P.M., 2017. Intertidal oysters reach their physiological limit in a future high-CO₂ world. *J. Exp. Biol.* 220, 765–774. <https://doi.org/10.1242/jeb.151365>.
- Smith, V.H., Jones II, T.P., Smith, M.S., 2005. Host nutrition and infectious disease: an ecological view. *Front. Ecol. Environ.* 3, 268–274. [https://doi.org/10.1890/1540-9295\(2005\)003\[0268:HNAIDA\]2.0.CO;2](https://doi.org/10.1890/1540-9295(2005)003[0268:HNAIDA]2.0.CO;2).
- Sokolova, I.M., 2013. Energy-limited tolerance to stress as a conceptual framework to integrate the effects of multiple stressors. *Integr. Comp. Biol.* 53, 597–608. <https://doi.org/10.1093/icb/ict028>.
- Sokolova, I., 2021. Bioenergetics in environmental adaptation and stress tolerance of aquatic ectotherms: linking physiology and ecology in a multi-stressor landscape. *J. Exp. Biol.* 224, jeb236802. <https://doi.org/10.1242/jeb.236802>.
- Sokolova, I.M., Frederich, M., Bagwe, R., Lannig, G., Sukhotin, A.A., 2012. Energy homeostasis as an integrative tool for assessing limits of environmental stress tolerance in aquatic invertebrates. *Mar. Environ. Res.* 79, 1–15. <https://doi.org/10.1016/j.marenvres.2012.04.003>.
- Steele, S., Mulcahy, M.F., 1999. Gametogenesis of the oyster *Crassostrea gigas* in southern Ireland. *J. Mar. Biol. Assoc. U. K.* 79, 673–686. <https://doi.org/10.1017/S0025315498000836>.
- Suquet, M., de Kermoyan, G., Araya, R.G., Queau, I., Lebrun, L., Souchu, P.L., Mingant, C., 2009. Anesthesia in Pacific oyster, *Crassostrea gigas*. *Aquat. Living Resour.* 22, 29–34. <https://doi.org/10.1051/alr/2009006>.
- Thomsen, J., Casties, I., Pansch, C., Körtzinger, A., Melzner, F., 2013. Food availability outweighs ocean acidification effects in juvenile *Mytilus edulis*: laboratory and field

- experiments. *Glob. Chang. Biol.* 19, 1017–1027. <https://doi.org/10.1111/gcb.12109>.
- Wallis, B., Smaal, A.C., Herman, P.M.J., Ysebaert, T., 2016. Niche dimension differs among life-history stages of Pacific oysters in intertidal environments. *Mar. Ecol. Prog. Ser.* 562, 113–122. <https://doi.org/10.3354/meps11961>.
- Wetz, M.S., Hutchinson, E.A., Lunetta, R.S., Paerl, H.W., Christopher Taylor, J., 2011. Severe droughts reduce estuarine primary productivity with cascading effects on higher trophic levels. *Limnol. Oceanogr.* 56, 627–638. <https://doi.org/10.4319/lo.2011.56.2.0627>.